Adipose tissue thickness and optical properties affect differential pathlength factor in NIRS studies on human skeletal muscle

Pirovano, Ileana, Porcelli, Simone, Re, Rebecca, Spinelli, Lorenzo, Contini, Davide, et al.

Ileana Pirovano, Simone Porcelli, Rebecca Re, Lorenzo Spinelli, Davide Contini, Mauro Marzorati, Alessandro Torricelli, "Adipose tissue thickness and optical properties affect differential pathlength factor in NIRS studies on human skeletal muscle," Proc. SPIE 11920, Diffuse Optical Spectroscopy and Imaging VIII, 119200T (9 December 2021); doi: 10.1117/12.2615254

SPIE.

Event: European Conferences on Biomedical Optics, 2021, Online Only

Adipose Tissue Thickness and Optical Properties Affect Differential Pathlength Factor in NIRS Studies on Human Skeletal Muscle

Ileana Pirovano[1], Simone Porcelli[1,2], Rebecca Re[3,4], Lorenzo Spinelli[4], Davide Contini[3], Mauro Marzorati[1], Alessandro Torricelli[3,4]

1 Istituto di Tecnologie Biomediche, Consiglio Nazionale delle Ricerche, via Fratelli Cervi 93, 20090, Segrate (Milan), Italy
2 Dipartimento di Medicina Molecolare, Università di Pavia, via Forlanini 6, 27100, Pavia, Italy
3 Dipartimento di Fisica, Politecnico di Milano, Piazza Leonardo da Vinci 32, 20133, Milan, Italy
4 Istituto di Fotonica e Nanotecnologie, Consiglio Nazionale delle Ricerche, Piazza Leonardo da Vinci 32, 20133, Milan, Italy
ileana.pirovano@itb.cnr.it

Abstract: We present simulation and *in-vivo* Time Domain NIRS studies to investigate differential pathlength factor in skeletal muscles at rest and its dependence on the subcutaneous adipose tissue thickness, tissue absorption and reduced scattering coefficients.

1. Introduction

Near Infra-Red Spectroscopy (NIRS) is a non-invasive technique that allows the assessment of oxidative metabolism in skeletal muscles [1], at rest and during exercise, by estimating the concentration of oxygenated and deoxygenated hemoglobin (O_2Hb and HHb) in the tissue. Most of the NIRS studies on skeletal muscles reported in the literature exploited the Continuous Wave (CW) technique, frequently using only one source-detector separation distance ρ. In this case, the simplest approach to retrieve O_2Hb and HHb concentrations changes over time relies on the modified Lambert-Beer Law. In this approach, a dimensionless wavelength-dependent coefficient, the Differential Pathlength Factor (DPF), is introduced to take into account that the photons pathlength in diffusive biological tissues is not equal to ρ because of scattering events [2]. A method to directly determine the DPF at wavelength λ is to employ Time Domain (TD) NIRS, which allows to record photons distribution of time-of flight (DTOF) and estimate the photons mean time-of-flight $\langle t(\lambda)\rangle$ inside the tissue. Together with the speed of light in vacuum c and the tissue refractive index $n(\lambda)$, it allows the calculation of the DPF by the following equation [3]:

$$DPF(\lambda) \cong \frac{1}{\rho} \cdot \frac{c}{n(\lambda)} \langle t(\lambda) \rangle \qquad (1)$$

When the time-of-flight information is not available, DPF values are usually taken from literature and kept constant for all subjects. However, there are only few works reporting the DPF of skeletal muscle [4,5] and it was suggested that the values could also depend on specific characteristics of the muscle itself and on the subcutaneous adipose tissue thickness (ATT). Moreover, since DPF may depend also on the measurement time, the wavelength, and the tissue optical properties, it is still not completely clear how the simplifying assumption of a constant DPF can affect the magnitude and the time-courses of the estimated O_2Hb and HHb concentrations [6]. In this work, we aim at evaluating in a quantitative and systematic way, by both simulations and an *in-vivo* study, the effect of ATT and tissue optical properties changes on the estimation of DPF in resting skeletal muscles.

2. Materials and Methods

2.1 Analytical simulations

A TD NIRS analytical simulation study was performed exploiting the solution of the Diffusion Equation for a bilayer model, thus mimicking a superficial layer composed by subcutaneous adipose tissue and a deeper layer corresponding to the skeletal muscle. Time-resolved reflectance curves were simulated for different combinations of absorption coefficient (μ_a), reduced scattering coefficient (μ'_s), and ATT. Eight different ATT values were tested *i.e.*, 1, 2, 2.5, 5, 7.5, 10, 12.5, 15 mm. Ranges of μ_a values (0.015 to 0.6 cm^{-1} in steps of 0.015 cm^{-1}) and μ'_s (3.5 to 12.5 cm^{-1} in steps of 0.5 cm^{-1}) were chosen. In the results, the subscript "0" identifies the properties of the first layer and subscript "1" ones of the second layer *i.e.*, μ_{a0}, μ'_{s0}, μ_{a1}, μ'_{s1}. To investigate separately the effect of optical properties variation in different layers, only one of the four parameters was changed at a time, for each ATT. For each combination of parameters, ten repeated DTOFs were generated with 10^6 photons/s, simulating two source-detector separation distances (a short ρ_s = 15 mm and a long one ρ_L = 30 mm). A constant background signal of 4 photons/channel was also simulated and a noise following the Poisson distribution was added to the theoretical model.

Diffuse Optical Spectroscopy and Imaging VIII, edited by Davide Contini, Yoko Hoshi, Thomas D. O'Sullivan, Proc. of SPIE-OSA Vol. 11920, 119200T · © 2021 OSA-SPIE
CCC code: 1605-7422/21/$21 · doi: 10.1117/12.2615254

2.2 *In-vivo measurements*

TD NIRS measurements in resting conditions of the *vastus lateralis* and the *biceps brachii* muscles of eleven healthy volunteers were performed after they signed an informed consent. The study was approved by the local Ethical Committee and conducted in accordance with the Declaration of Helsinki. Subjects had an average (± SD) age of 28.5 ± 6.8 years and a similar level of physical activity. Measurements of the subcutaneous ATT above the probed region were taken with a skin fold caliper. Data were collected during 60 s of resting phase and repeated three times for each muscle. A TD NIRS medical device designed for muscles probing was employed [7]. The same wavelength and ρ used for the simulation study were chosen. A 3D printed custom probe was positioned on the left leg (or arm) and fixed with an adhesive black bandage, thus preventing motion artifacts, and shielding from the background light.

Both in the simulation study and in the *in-vivo* experiments, the DPF was calculated by Eq. (1). For *in-vivo* data analysis, this calculation was repeated for the signal acquired at each wavelength, each source-detector separation distance and for every time of acquisition of both leg and arm of each subject.

3. Results

3.1 Analytical simulations

In Fig. 1 (a) and (b), the DPF values obtained by simulations are reported as a function of the changing optical properties in the two layers. A non-linear decrease is observed when μ_{a0} and μ_{a1} increase (first row). This is particularly accentuated for variations of the deeper layer and for larger ATT. On the contrary, the DPF increases with increasing μ'_{s0} and μ'_{s1} (second raw), grater variations are observed when the superficial scattering properties are changing, and a non-linear trend is observed for smaller ATT (< 5 mm). In Fig. 1 (c) and (d), the DPF is represented as a function of ATT. The DPF shows an increasing trend with ATT for lower μ_{a0} and a decreasing trend for higher μ_{a0}. For ATT < 5 mm and μ_{a0} = 0.15 cm^{-1}, the DPF is quite constant and the dependence on μ_{a0} and μ'_{s0} is less evident. Opposite behavior is observed when μ_{a1} and μ'_{s1} vary. Finally, a DPF increasing trend with ATT is observed when the absorption is kept constant and reduced scattering coefficient changes (second raw).

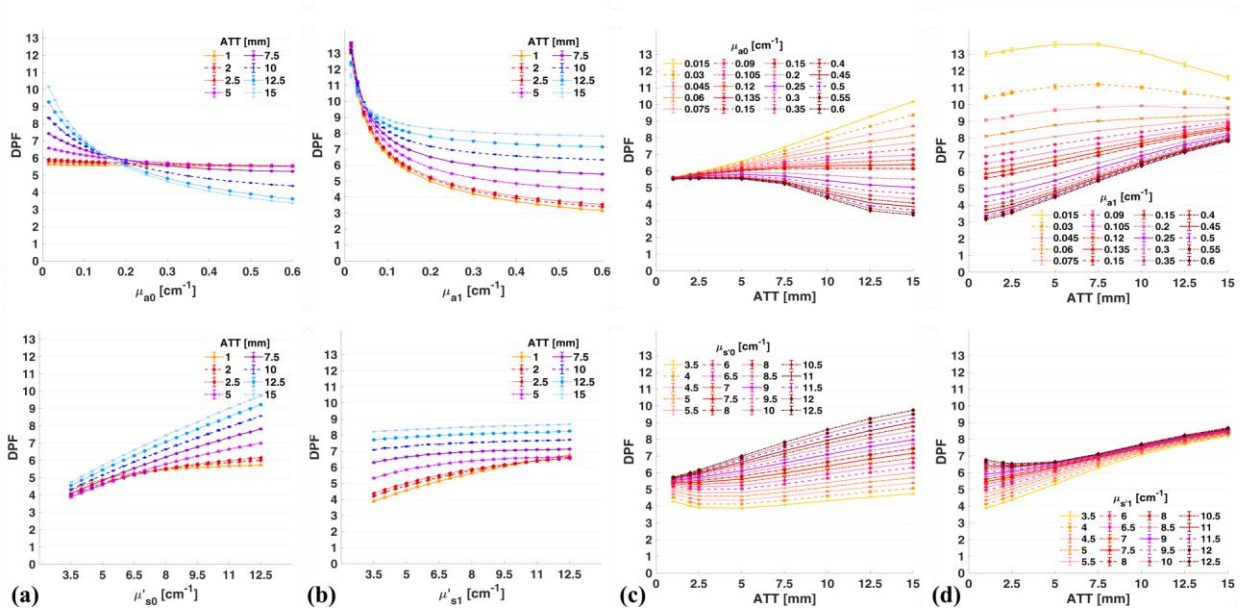

Fig. 1. DPF (dot: average of 10 values, bars: standard deviations) obtained for simulated DTOF at ρ_L = 30 mm. (a) and (b): DPF as function of μ_a and μ'_s of the first and second layer, for the different ATT. (c) and (d): DPF against ATT for varying μ_a and μ'_s of the two layers.

3.2 *In-vivo measurements*

A considerable variation between subjects is observed, with values ranging from 2.9 to 6.1 for legs and from 2.8 to 5.0 for arms. Moreover, a significant difference between the muscles of the same subject is found (Wilcoxon rank sum test, 0.02 < p-values < 0.05). In general, higher DPF values for the *vastus lateralis* muscles (4.62±0.84 at 690 nm and 4.19±0.80 at 830 nm, ρ_L = 30 mm) with respect to the *biceps brachii* ones (3.80±0.53 at 690 nm and 3.49±0.53 at 830 nm, ρ_L = 30 mm) is observed. The DPF

calculated at 830 nm appears to be significantly smaller than the one at 690 nm (Wilcoxon signed-rank test, p-values < 0.001). No significant influence of source-detector separation distances on the DPFs can be observed. In Fig. 2, the relationship between DPF and ATT for the *vastus lateralis* is reported. A positive correlation between the DPF and the subcutaneous thickness can be observed at all wavelengths and ρ (0.85 < Pearson's R < 0.94 and p-value < 0.001). This relationship is also well represented by linear trend lines, whose equations have positive 1st order coefficients. On the contrary, no significant correlation is found in the *biceps brachii*, probably because of the small ATT range available (from 1.2 to 2.3 mm).

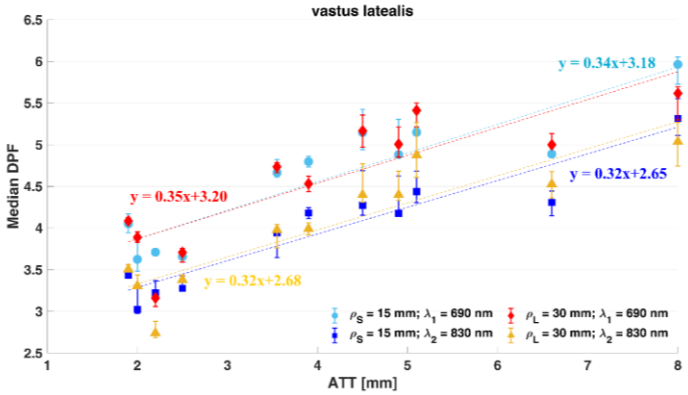

Fig. 2. *In-vivo* v*astus lateralis* DPFs median values (dots) against the ATT of each subject, each wavelength and source-detector separation combination. Bars represent the maximum and minimum deviation from the median value. Trend lines for each series ($0.73 < R^2 < 0.88$) are superimposed.

4. Discussion and Conclusions

Considering the key role of DPF in retrieving the variations of O_2Hb and HHb concentrations by the modified Lambert-Beer law, its accurate and actual determination is crucial. From systematic simulations, we observe that the DPF value is affected by the optical properties of both the subcutaneous adipose tissue and the deeper skeletal muscle, especially for thicker ATTs. From TD NIRS *in-vivo* measurements on two skeletal muscles at rest, DPF differences are found among each subject and different muscles. Moreover, the non-linear behavior observed for the DPF in simulated situations when the optical properties changed, suggests that even the DPF of the same limb can dynamically change over time. For example, during exercise, when the absorption and reduced scattering coefficients of the muscles change due to variation of the oxygen consumption and structure organization of the tissue itself. These results suggest that a personalized time-dependent DPF should be calculated and considered.

5. Acknowledgment

This work was supported by Regione Lombardia and Fondazione Cariplo in the framework of the project EMPATIA@Lecco - EMpowerment del PAzienTe In cAsa - Rif. 2016-1428.

6. References

[1] B. Grassi and V. Quaresima, "Near-infrared spectroscopy and skeletal muscle oxidative function in vivo in health and disease: a review from an exercise physiology perspective," J. Biomed. Opt. **21**(9), 091313 (2016).

[2] M. Essenpreis, M. Cope, C. E. Elwell, S. R. Arridge, P. van der Zee, and D. T. Delpy, "Wavelength depencence of the differential pathlength factor and the log slope in time-resolved tissue spectroscopy," in *Optical Imaging of Brain Function and Metabolism*, P. U. Dirnagl, A. Villringer, and K. M. Einhäupl, Eds., ed. (Springer Science+Business Media New York, 1993), p. 9.20.

[3] F. Scholkmann, S. Kleiser, A. J. Metz, R. Zimmermann, J. Mata Pavia, U. Wolf, and M. Wolf, "A review on continuous wave functional near-infrared spectroscopy and imaging instrumentation and methodology," Neuroimage **85**, 6–27 (2014)

[4] A. Duncan, J. H. Meek, M. Clemence, C. E. Elwell, L. Tyszczuk, M. Cope, and D. Delpy, "Optical pathlength measurements on adult head, calf and forearm and the head of the newborn infant using phase resolved optical spectroscopy," Phys. Med. Biol. **40**(2), 295–304 (1995).

[5] U. Wolf, M. Wolf, J. H. Choi, L. A. Paunescu, L. P. Safonova, A. Michalos, and E. Gratton, "Mapping of hemodynamics on the human calf with near infrared spectroscopy and the influence of the adipose tissue thickness," Adv. Exp. Med. Biol. **510**, 225–230 (2003).

[6] A. M. Chiarelli, D. Perpetuini, C. Filippini, D. Cardone, and A. Merla, "Differential pathlength factor in continuous wave functional near-infrared spectroscopy: reducing hemoglobin's cross talk in high-density recordings," Neurophotonics **6**(03), 1 (2019).

[7] R. Re, I. Pirovano, D. Contini, L. Spinelli, and A. Torricelli, "Time Domain Near Infrared Spectroscopy Device for Monitoring Muscle Oxidative Metabolism: Custom Probe and In Vivo Applications," Sensors **18**, 264 (2018)